Since January 2020 Elsevier has created a COVID-19 resource centre with free information in English and Mandarin on the novel coronavirus COVID-19. The COVID-19 resource centre is hosted on Elsevier Connect, the company's public news and information website.

JACC: CARDIOVASCULAR IMAGING VOL. 13, NO. 11, 2020

PUBLISHED BY ELSEVIER

ORIGINAL RESEARCH

Prognostic Value of Right Ventricular Longitudinal Strain in Patients With COVID-19

Yuman Li, MD, PhD,* He Li, MD, PhD,* Shuangshuang Zhu, MD,* Yuji Xie, MD,* Bin Wang, MD, Lin He, MD, PhD, Danqing Zhang, MD, Yongxing Zhang, MD, Hongliang Yuan, MD, Chun Wu, MD, PhD, Wei Sun, MD, Yanting Zhang, MD, Meng Li, MD, Li Cui, MD, Yu Cai, MD, Jing Wang, MD, PhD, Yali Yang, MD, PhD, Qing Lv, MD, PhD, Li Zhang, MD, PhD, Mingxing Xie, MD, PhD

ABSTRACT

OBJECTIVES The aim of this study was to investigate whether right ventricular longitudinal strain (RVLS) was independently predictive of higher mortality in patients with coronavirus disease-2019 (COVID-19).

BACKGROUND RVLS obtained from 2-dimensional speckle-tracking echocardiography has been recently demonstrated to be a more accurate and sensitive tool to estimate right ventricular (RV) function. The prognostic value of RVLS in patients with COVID-19 remains unknown.

METHODS One hundred twenty consecutive patients with COVID-19 who underwent echocardiographic examinations were enrolled in our study. Conventional RV functional parameters, including RV fractional area change, tricuspid annular plane systolic excursion, and tricuspid tissue Doppler annular velocity, were obtained. RVLS was determined using 2-dimensional speckle-tracking echocardiography. RV function was categorized in tertiles of RVLS.

RESULTS Compared with patients in the highest RVLS tertile, those in the lowest tertile were more likely to have higher heart rate; elevated levels of D-dimer and C-reactive protein; more high-flow oxygen and invasive mechanical ventilation therapy; higher incidence of acute heart injury, acute respiratory distress syndrome, and deep vein thrombosis; and higher mortality. After a median follow-up period of 51 days, 18 patients died. Compared with survivors, nonsurvivors displayed enlarged right heart chambers, diminished RV function, and elevated pulmonary artery systolic pressure. Male sex, acute respiratory distress syndrome, RVLS, RV fractional area change, and tricuspid annular plane systolic excursion were significant univariate predictors of higher risk for mortality ($p < 0.05$ for all). A Cox model using RVLS (hazard ratio: 1.33; 95% confidence interval [CI]: 1.15 to 1.53; $p < 0.001$; Akaike information criterion = 129; C-index = 0.89) was found to predict higher mortality more accurately than a model with RV fractional area change (Akaike information criterion = 142, C-index = 0.84) and tricuspid annular plane systolic excursion (Akaike information criterion = 144, C-index = 0.83). The best cutoff value of RVLS for prediction of outcome was −23% (AUC: 0.87; $p < 0.001$; sensitivity, 94.4%; specificity, 64.7%).

CONCLUSIONS RVLS is a powerful predictor of higher mortality in patients with COVID-19. These results support the application of RVLS to identify higher risk patients with COVID-19. (J Am Coll Cardiol Img 2020;13:2287–99)

From the Department of Ultrasound, Union Hospital, Tongji Medical College, Huazhong University of Science and Technology, Wuhan, China; and the Hubei Province Key Laboratory of Molecular Imaging, Wuhan, China. *Drs. Y. Li, H. Li, S. Zhu, and Y. Xie contributed equally to this work.

The authors attest they are in compliance with human studies committees and animal welfare regulations of the authors' institutions and Food and Drug Administration guidelines, including patient consent where appropriate. For more information, visit the *JACC: Cardiovascular Imaging* author instructions page.

Manuscript received April 8, 2020; revised manuscript received April 23, 2020, accepted April 24, 2020.

ISSN 1936-878X/$36.00 https://doi.org/10.1016/j.jcmg.2020.04.014

ABBREVIATIONS AND ACRONYMS

2D = 2-dimensional

AIC = Akaike information criterion

ARDS = acute respiratory distress syndrome

CI = confidence interval

COVID-19 = coronavirus disease-2019

HR = hazard ratio

LS = longitudinal strain

LV = left ventricular

LVEF = left ventricular ejection fraction

PASP = pulmonary artery systolic pressure

ROC = receiver-operating characteristic

RV = right ventricular

RVFAC = right ventricular fractional area change

RVLS = right ventricular longitudinal strain

S' = tricuspid lateral annular systolic velocity

SARS-CoV-2 = severe acute respiratory syndrome-coronavirus-2

STE = speckle-tracking echocardiography

TAPSE = tricuspid annular plane systolic excursion

TR = tricuspid regurgitation

Coronavirus disease-2019 (COVID-19), caused by severe acute respiratory syndrome-coronavirus-2 (SARS-CoV-2), has reached more than 170 countries, resulting in considerable morbidity and mortality. Although currently available studies have confirmed the presence of myocardial injury and its association with mortality in patients with COVID-19 (1,2), they lack evidence from echocardiography to determine the features of cardiac injury. As the prevalence of acute respiratory distress syndrome (ARDS) has been reported to be 29% to 67% among critically ill patients with COVID-19 (3,4), right ventricular (RV) function is presumed to be more susceptible to impairment because of increased RV afterload. In clinical practice, RV structure and function are evaluated mainly using echocardiography. The conventional echocardiographic parameters have limited diagnostic value, as they may fail to detect early abnormalities of RV systolic function (5). Recently, 2-dimensional (2D) speckle-tracking echocardiography (STE), which evaluates myocardial function accurately and reproducibly (6,7), has been introduced. Because of its capability to detect subclinical impairment of cardiac function, 2D STE has been extensively applied to investigate RV function in different clinical settings (8–10). Moreover, RV longitudinal strain (RVLS) derived from 2D STE has been demonstrated to be of prognostic value (11). To the best of our knowledge, there are no data regarding the use of RVLS in patients with COVID-19. In addition, confirming the role of RVLS in these patients may be of additional significance, as most patients exhibit preserved conventional echocardiographic parameters, and thus detection and risk stratification among these patients may be challenging. Accordingly, the purpose of this study was to evaluate the prognostic value of RVLS in patients with COVID-19.

METHODS

STUDY POPULATION. This observational study was performed at the west branch of Union Hospital, Tongji Medical College, Huazhong University of Science and Technology, a designated hospital to treat patients with COVID-19. We included a total of 150 consecutive adult patients with COVID-19 who were diagnosed according to the interim guidance of the World Health Organization (12) from February 12, 2020, to March 15, 2020. Considering the presence of cardiac damage in patients with COVID-19, bedside echocardiography was performed in all patients from 3 wards managed by the investigators for the evaluation of cardiac function. The median time from admission to echocardiography was 7 days (interquartile range: 3 to 10 days). Patients with known cardiomyopathy, previous myocardial infarction, or suboptimal images were excluded. Of these patients, 2 had dilated cardiomyopathy, 4 had old myocardial infarction, and 24 did not have images of sufficient quality for echocardiographic analysis. The remaining 120 patients were included in our final analysis. The control group consisted of 37 healthy volunteers who had no cardiopulmonary disease on the basis of physical examination, electrocardiography, chest radiography, and echocardiography.

The study complied with the edicts of the 1975 Declaration of Helsinki (13) and was approved by the institutional ethics board of Union Hospital Tongji Medical College, Huazhong University of Science and Technology (20200022). The requirement to obtain written informed consent was waived for all participants with emerging infectious diseases.

CLINICAL DATA. Patients' demographic characteristics, medical histories, laboratory examinations, comorbidities, complications, treatments, and outcomes were retrieved from electronic medical records. Cardiac biomarkers measured on admission included hypersensitive troponin I, creatine kinase muscle-brain, and B-type natriuretic peptide. These data were independently reviewed and entered into the computer database by 2 analysts (C.W. and W.S.) The final follow-up date was April 2, 2020.

TRANSTHORACIC ECHOCARDIOGRAPHY. Bedside transthoracic echocardiographic examinations were performed in all patients using the EPIQ 7C ultrasound system (Philips Medical Systems, Andover, Massachusetts). Two-dimensional and Doppler echocardiography were performed on the basis of the guidelines of the American Society of Echocardiography (14). Images were stored and analyzed by 2 independent observers (Y.C. and L.C.) blinded to clinical data.

CONVENTIONAL ECHOCARDIOGRAPHIC ANALYSIS. Left ventricular (LV) end-systolic volume and end-diastolic volume and LV ejection fraction (LVEF) were measured using the biplane Simpson method (15). LV mass was calculated from the parasternal view on the basis of Devereux's formula. LV diastolic function was estimated using the ratio of early transmitral flow velocity (E) to late

transmitral flow velocity (A) and the ratio of transmitral E to early diastolic medial LV septal tissue velocity (e′).

Right atrial and RV size were determined from the apical 4-chamber view. Tricuspid annular plane systolic excursion (TAPSE) was measured as the systolic displacement of the tricuspid lateral annulus, recorded on M-mode imaging. RV end-diastolic and end-systolic areas were obtained from the apical 4-chamber view. RV fractional area change (RVFAC) was calculated as: (RV end-diastolic area − RV end-systolic area)/end-diastolic area × 100%. Tricuspid lateral annular systolic velocity (S′) was assessed using tissue Doppler imaging from the apical 4-chamber view. Estimation of tricuspid regurgitation (TR) incorporated color Doppler imaging and contour of the jet on continuous-wave Doppler imaging. Moderate to severe TR was defined as moderate, moderate to severe, or severe TR. Pulmonary artery systolic pressure (PASP) was assessed from the peak velocity of the TR jet, using the modified Bernoulli equation plus right atrial pressure evaluated from the inferior vena cava size and its collapsibility.

SPECKLE-TRACKING ECHOCARDIOGRAPHIC ANALYSIS. STE was conducted according to the recommendations of the American Society of Echocardiography and the European Association of Cardiovascular Imaging (6). All of the images were analyzed using 2D AutoStrain software (Qlab13, Philips Healthcare, Andover, Massachusetts) in the apical 4-chamber view at a frame rate of 50 to 70 frames/s (**Figure 1**). After tracing the RV endocardial border, the region of interest was automatically generated. Manual corrections were then performed to fit RV myocardial wall thickness. The RV free wall was automatically divided into 3 segments: basal, mid, and apical. RVLS was calculated as the mean of the strain values in the 3 segments of the RV free wall. If it was not feasible to track 1 or more segments, the case was excluded. We took the absolute value for a simpler interpretation, as RVLS is a negative value.

INTEROBSERVER AND INTRAOBSERVER REPRODUCIBILITY. Intraobserver and interobserver variability of RVLS was estimated in 20 randomly selected subjects and evaluated using intraclass correlation coefficients and Bland-Altman analysis. Intraobserver variability was assessed by having 1 observer remeasure after 2 weeks. Interobserver variability was evaluated by a second observer who was blinded to the first observer's measurements.

STATISTICAL ANALYSIS. Continuous numeric variables are expressed as mean ± SD or median (interquartile range) and were compared using a 2-sample Student's *t*-test and 1-way analysis of variance (for normally distributed data) or the Mann-Whitney *U* test and Kruskal-Wallis test (for non-normally distributed data). Categorical variables are expressed as frequency (percentage) and were compared using the chi-square test or the Fisher exact test. To determine the optimal cutoff value (maximum Youden index) of prognostic RV functional parameters for detecting increased mortality, receiver-operating characteristic (ROC) curves were used. Survival curves were obtained in a Kaplan-Meier analysis and compared using the log-rank test. Estimations of the predictors of mortality were performed using univariate and multivariate Cox regression models. All potential predictors of higher mortality were entered into univariate analyses, including sex, age, cardiac injury and inflammatory markers, LVEF, PASP, RV functional echocardiographic parameters, ARDS, and comorbidities (diabetes mellitus, hypertension, cardiovascular artery disease, malignancy, and arrhythmia). Variables with p values <0.05 in univariate analysis were entered into multivariate Cox regression models. For multivariate analysis, a separate Cox proportional hazards model including clinical variables and 1 of the RV function parameters (TAPSE, RVFAC, or RVLS) was used to determine the independent predictors of higher mortality. Model performance was assessed using the Akaike information criterion (AIC) and the C-index. Data were analyzed using SPSS version 24.0 (SPSS Inc., Chicago, Illinois), MedCalc Version 19.0.4 (MedCalc Software, Ostend, Belgium), and R version 3.6.3 (R Foundation for Statistical Computing, Vienna, Austria). A 2-sided p value <0.05 was considered to indicate statistical significance.

RESULTS

CLINICAL CHARACTERISTICS. Clinical characteristics of patients with COVID-19 according to tertiles of RVLS are shown in **Table 1**. The mean age of patients with COVID-19 was 61 ± 14 years, and 57 (48%) were men. Chronic obstructive pulmonary disease was found in 6 patients with COVID-19. None of the patients had histories of pulmonary embolism. No patient was diagnosed with pulmonary embolism. Compared with patients in the highest tertiles, those in the lowest RVLS tertile were more likely to have higher heart rates; elevated levels of D-dimer and C-reactive protein; more high-flow oxygen and invasive mechanical ventilation therapy; higher incidence of acute heart injury, ARDS, and deep vein thrombosis;

FIGURE 1 RVLS Obtained From 2-Dimensional Speckle Tracking Echocardiography in Patients With COVID-19

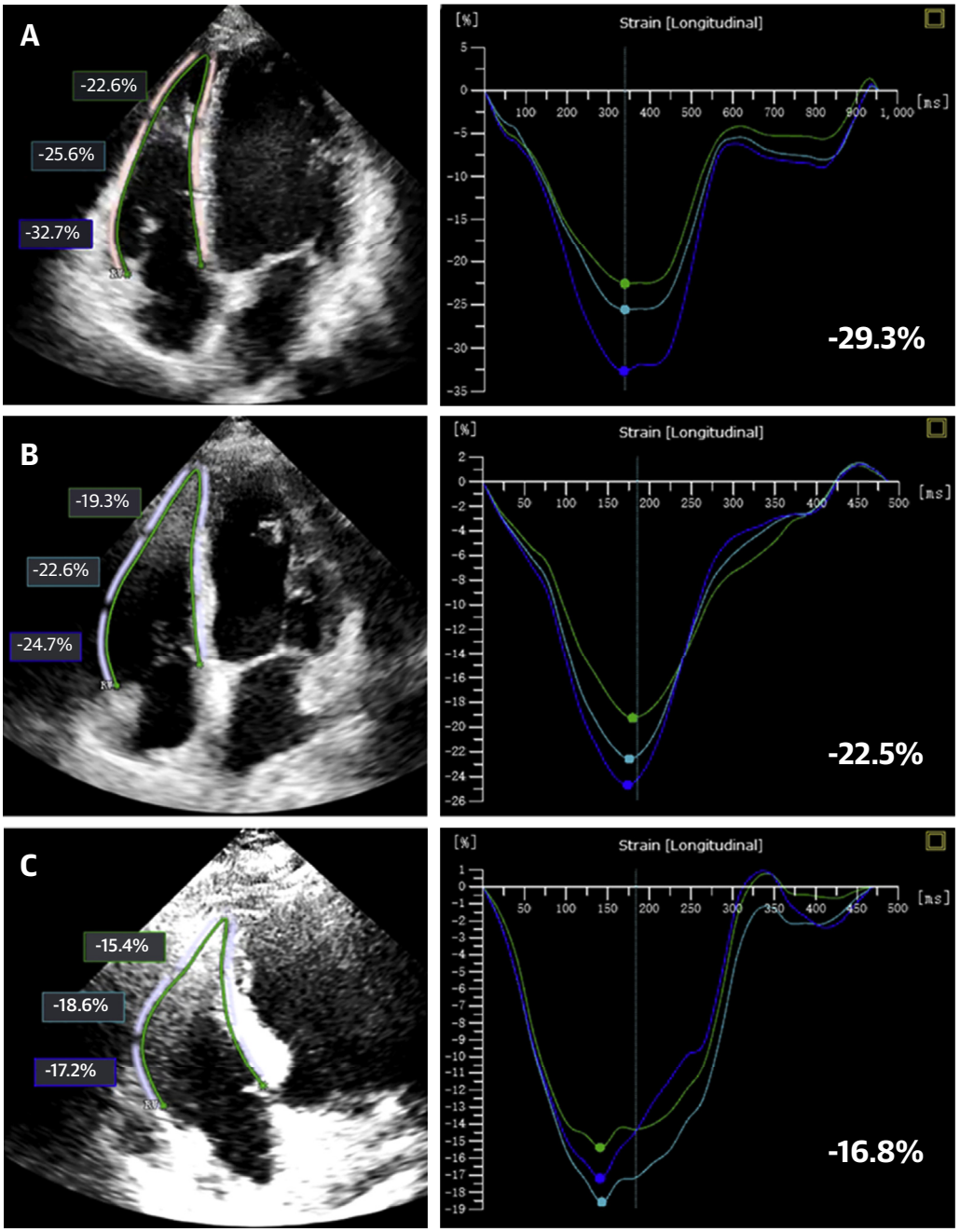

(A) Representative images of the highest tertile of right ventricular longitudinal strain (RVLS). **(B)** Representative images of the middle tertile of RVLS. **(C)** Representative images of the lowest tertile of RVLS.

and higher mortality. There were no significant differences in age, sex, systemic arterial pressure, comorbidities, lymphocyte count, levels of creatine kinase muscle-brain, hypersensitive troponin I and B-type natriuretic peptide, partial pressure of oxygen/fraction of inspiration oxygen, procalcitonin, antiviral, antibiotic, glucocorticoid, and angiotensin-converting enzyme inhibitor or angiotensin II

TABLE 1 Clinical Characteristics of Patients With COVID-19 According to Tertiles of RVLS

	Total Population: RVLS 10.3%-35.7% (N = 120)	Upper Tertile: RVLS 25.5%-35.7% (n = 40)	Middle Tertile: RVLS 20.6%-25.4% (n = 40)	Lower Tertile: RVLS 10.3%-20.5% (n = 40)	p Value
Clinical characteristics					
Age, yrs	61 ± 14	61 ± 14	57 ± 15	64 ± 13	0.102
Male	57 (48)	19 (48)	16 (40)	22 (55)	0.412
Body mass index, kg/m^2	23.7 ± 3.0	24.1 ± 3.2	23.0 ± 3.1	23.8 ± 2.8	0.337
Heart rate, beats/min	92 ± 17	87 ± 17	91 ± 17	96 ± 17*	0.066
Respiratory rate, breaths/min	26 ± 9	25 ± 5	27 ± 13	27 ± 6	0.607
Systolic arterial pressure, mm Hg	130 ± 22	131 ± 22	129 ± 29	132 ± 19	0.812
Diastolic arterial pressure, mm Hg	80 ± 14	82 ± 11	79 ± 18	81 ± 12	0.623
Smoking	6 (5.0)	2 (5.0)	1 (2.5)	3 (7.5)	0.611
Comorbidities					
Hypertension	48 (40)	12 (30)	16 (40)	20 (50)	0.192
Diabetes	14 (11.7)	5 (12.5)	4 (10.0)	5 (12.5)	0.924
Obesity	22 (18.3)	8 (20.0)	6 (15.0)	6 (15.0)	0.799
COPD	6 (5.0)	3 (7.5)	0 (0.0)	3 (7.5)	0.210
Coronary artery disease	11 (9.2)	3 (7.5)	3 (7.5)	5 (12.5)	0.689
Chronic kidney disease	17 (14.2)	3 (7.5)	6 (15.0)	8 (20.0)	0.369
Chronic liver disease	4 (3.3)	2 (5.0)	2 (5.0)	0 (0.0)	0.375
Malignancy	8 (6.7)	3 (7.5)	4 (10.0)	1 (2.5)	0.398
Laboratory findings					
Lymphocyte count, $\times 10^9$/l	1.08 ± 0.61	1.14 ± 0.48	1.04 ± 0.67	1.05 ± 0.66	0.755
D-dimer, mg/l	1.45 (0.50–4.91)	0.76 (0.35–2.64)	2.10 (0.49–6.72)*	1.84 (0.83–6.13)*	0.053
CK-MB, U/l	9 (4.5–13.5)	9 (4.5–13.5)	9 (5.0–11.3)	12 (4.5–20.0)	0.256
hs-TNI, ng/l	3.5 (1.8–14.4)	2.4 (1.1–4.7)	3.5 (1.6–9.3)	10.8 (2.6–59.5)	0.330
BNP, pg/ml	53.1 (28.2–131.4)	51.4 (28.0–90.9)	52.6 (39.4–124.7)	86.1 (24.2–232.7)	0.518
PaO_2/FiO_2, mm Hg	217.8 (152.1–256.8)	254.1 (221.9–287.9)	167.5 (152.7–269.6)	178.8 (140.4–210.8)	0.282
CRP, mg/l	24.0 (2.8–65.1)	11.2 (1.1–48.7)	23.4 (3.6–71.8)	29.8 (3.7–64.2)*	0.053
PCT, ng/ml	0.15 (0.06–0.24)	0.11 (0.05–0.22)	0.13 (0.05–0.26)	0.16 (0.10–0.25)	0.557
Treatments					
Antiviral therapy	112 (93.3)	38 (95.0)	37 (92.5)	37 (92.5)	0.877
Antibiotic therapy	85 (70.8)	25 (62.5)	28 (70.0)	32 (80.0)	0.229
Glucocorticoid therapy	46 (38.3)	12 (30.0)	13 (32.5)	21 (52.5)	0.077
ACE inhibitor/ARB	8 (6.7)	3 (7.5)	1 (2.5)	4 (10.0)	0.398
Oxygen therapy	105 (87.5)	35 (87.5)	36 (90.0)	34 (85.0)	0.800
High-flow oxygen	58 (48.3)	16 (40.0)	16 (40.0)	26 (65.0)*†	0.035
IMV	15 (12.5)	0 (0.0)	5 (12.5)*	10 (25.0)*	0.003
NIMV	6 (5.0)	1 (2.5)	2 (5.0)	3 (7.5)	0.593
ICU admission	22 (21.0)	4 (10.0)	8 (20.0)	10 (25.0)	0.214
Complications					
Acute kidney injury	16 (13.0)	3 (7.5)	5 (12.5)	8 (20.0)	0.259
Acute heart injury	37 (30.8)	5 (12.5)	10 (25.0)*	22 (55.0)*†	<0.001
ARDS	41 (34.2)	10 (25.0)	10 (25.0)	21 (52.5)*†	0.011
DVT	49 (41.0)	12 (30.0)	12 (30.0)	25 (62.5)*†	0.003
Prognosis					
Hospital stay	3 (2.5)	0 (0.0)	2 (5.0)	1 (2.5)	0.371
Discharge	99 (82.5)	40 (100.0)	33 (82.5)	26 (65.0)*	0.077
Death	18 (15.0)	0 (0.0)	5 (12.5)*	13 (32.5)*†	<0.001

Values are mean ± SD, n (%), or median (interquartile range). *$p < 0.05$, lowest or middle tertiles vs. highest RVLS tertile. †$p < 0.05$, lowest tertile vs. middle RVLS tertile.

ACE = angiotensin-converting enzyme; ARB = angiotensin II receptor blocker; ARDS = acute respiratory distress syndrome; BNP = B-type natriuretic peptide; CK-MB = creatine kinase muscle-brain; COPD = chronic obstructive pulmonary disease; COVID-19 = coronavirus disease-2019; CRP = C-reactive protein; FiO_2 = fraction of inspiration oxygen; DVT = deep vein thrombosis; hs-TNI = hypersensitive troponin I; ICU = intensive care unit; IMV = invasive mechanical ventilation; NIMV = noninvasive mechanical ventilation; PCT = procalcitonin; PaO_2 = partial pressure of oxygen; RVLS = right ventricular longitudinal strain.

TABLE 2 Echocardiographic Characteristics of Patients With COVID-19 According to Tertiles of RVLS

	Total Population: RVLS 10.3%-35.7% (N = 120)	Upper Tertile: RVLS 25.5%-35.7% (n = 40)	Middle Tertile: RVLS 20.6%-25.4% (n = 40)	Lower Tertile: RVLS 10.3%-20.5% (n = 40)	p Value
Left heart					
LA dimension, mm	34.3 ± 5.4	35.2 ± 3.9	32.9 ± 4.6	34.7 ± 6.9	0.141
LV dimension, mm	45.3 ± 4.8	45.7 ± 4.0	44.6 ± 5.7	45.6 ± 4.6	0.549
LV mass, g/m^2	140.1 ± 32.8	141.0 ± 29.8	134.0 ± 36.0	145.2 ± 32.3	0.320
E/A ratio	0.9 ± 0.3	0.9 ± 0.3	0.9 ± 0.3	0.9 ± 0.4	0.944
E/e′ ratio	9.1 ± 3.1	8.8 ± 3.3	8.6 ± 2.2	9.7 ± 3.6	0.265
LVEDV, ml	85.4 ± 25.1	90.1 ± 21.8	80.7 ± 26.4	85.1 ± 27.0	0.295
LVESV, ml	32.8 ± 13.5	35.9 ± 11.5	29.8 ± 10.8*	32.9 ± 17.2	0.199
LVEF, %	63.4 ± 7.0	62.0 ± 5.9	64.3 ± 6.4	63.9 ± 8.4	0.315
Right heart					
RA dimension, mm	35.4 ± 4.7	34.7 ± 3.5	34.2 ± 3.6	37.3 ± 6.2*†	0.013
RV dimension, mm	33.6 ± 4.2	33.0 ± 3.8	33.1 ± 3.8	34.8 ± 5.1	0.102
PA, mm	23.5 ± 2.8	23.4 ± 1.7	23.1 ± 2.8	24.0 ± 3.6	0.440
IVC, mm	15.6 ± 3.6	16.1 ± 3.7	15.4 ± 3.6	15.2 ± 3.4	0.591
RVLS, %	23.5 ± 4.7	28.6 ± 2.9	23.5 ± 1.4*	18.4 ± 1.8*†	<0.001
RVFAC, %	45.8 ± 6.1	47.5 ± 5.3	45.9 ± 6.4	43.9 ± 6.0*	0.026
TAPSE, mm	22.9 ± 3.6	23.8 ± 3.5	23.0 ± 3.7	21.8 ± 3.4*	0.046
S′, cm/s	13.6 ± 2.4	13.6 ± 2.7	13.3 ± 2.4	13.9 ± 2.2	0.461
Moderate to severe TR	8 (6.7)	1 (2.5)	3 (7.5)	4 (10.0)*	0.398
PASP, mm Hg	31 (22-45)	27 (24-37)	32 (24-46)	32 (25-48)*	0.311

Values are mean ± SD, n (%), or median (interquartile range). RVLS values are absolute values. *p < 0.05, lowest or middle tertile vs. highest RVLS tertile. †p < 0.05, lowest tertile vs. middle RVLS tertile.

IVC = inferior vena cava; LA = left atrial; LV = left ventricular; LVEDV = left ventricular end-diastolic volume; LVESV = left ventricular end-systolic volume; LVEF = left ventricular ejection fraction; PA = pulmonary artery; PASP = pulmonary artery systolic pressure; RA = right atrial; RV = right ventricular; RVFAC = fractional area change; RVLS = right ventricular longitudinal strain; TAPSE = tricuspid annular plane systolic excursion; TR = tricuspid regurgitation.

receptor blocker use, number of intensive care unit admissions, and acute kidney injury among the tertiles.

ECHOCARDIOGRAPHIC CHARACTERISTICS. Echocardiographic characteristics of patients with COVID-19 are described in Tables 2 and 3. Compared with patients in the highest RVLS tertiles, those in the lowest tertile had similar left atrial and LV size, LV mass, E/A ratio, E/e′ ratio, LV end-diastolic volume, LV end-systolic volume, and LVEF. The distribution of RVLS in patients with COVID-19 is presented in Figure 2. Patients in the lowest RVLS tertile exhibited dilated right atrium; lower RVLS, RVFAC, and TAPSE; more moderate to severe TR; and higher PASP. However, RV, pulmonary artery, and inferior vena cava dimensions and S′ did not differ among the tertiles. RVLS was lower in patients with ARDS than in those without ARDS (21.3 ± 4.6% vs. 24.6 ± 4.4%; p < 0.001).

After a median follow-up period of 51 days, 18 patients had died. Left heart structure (left atrial and LV end-diastolic dimensions, LV mass and volumes) and LV systolic (LVEF) and diastolic (E/A ratio, E/e′ ratio) function were not different between nonsurvivors and survivors. Compared with survivors, nonsurvivors displayed enlarged right heart chambers and pulmonary arteries; lower RVLS, RVFAC, and TAPSE; and elevated PASP. Inferior vena cava diameter, moderate to severe TR, and S′ were similar in survivors and nonsurvivors.

PREDICTORS OF MORTALITY IN PATIENTS WITH COVID-19. RVLS and conventional RV function indexes were entered into an ROC analysis to estimate the probability of poor clinical outcome. RVLS, RVFAC, and TAPSE were associated with higher mortality (Figure 3). Area under the curve for RVLS (0.87) was greater than that for RVFAC (0.72; p = 0.028) and TAPSE (0.67; p = 0.002). Therefore, RVLS most accurately predicted higher risk for mortality. Optimal cutoff values of RV function parameters for identifying higher mortality were 23% for RVLS, 43.5% for RVFAC, and 23 mm for TAPSE. The best cutoff value of RVLS for detection of increased mortality was 23%, with sensitivity of 94.4% and specificity of 64.7%.

Figure 4 and the Central Illustration show Kaplan-Meier survival curves for mortality. Among the patients, when separated by tertiles, mortality was highest in patients with RVLS ≤20.5%, followed by RVLS in the range between 20.6% and 25.4%, and

TABLE 3 Echocardiographic Characteristics of Survivors and Nonsurvivors With COVID-19

	All Patients (N = 120)	Survivors (n = 102)	Nonsurvivors (n = 18)	p Value
Left heart				
LA dimension, mm	34.3 ± 5.4	34.2 ± 5.1	34.7 ± 6.7	0.696
LV dimension, mm	45.3 ± 4.8	45.4 ± 4.9	44.8 ± 4.2	0.649
LV mass, g/m^2	142.8 ± 31.4	139.6 ± 33.2	142.8 ± 31.4	0.710
E/A ratio	0.29 ± 0.35	0.92 ± 0.36	0.93 ± 0.30	0.902
E/e′ ratio	9.1 ± 3.1	9.0 ± 3.2	9.4 ± 3.0	0.677
LVEDV, ml	85.6 ± 24.2	87.1 ± 25.2	78.3 ± 17.4	0.138
LVESV, ml	24.8 ± 5.7	25.1 ± 5.8	23.8 ± 5.4	0.106
LVEF, %	63.4 ± 7.0	63.0 ± 7.0	65.8 ± 6.7	0.135
Right heart				
RA dimension, mm	35.4 ± 4.7	34.8 ± 4.2	38.6 ± 6.0	0.001
RV dimension, mm	33.6 ± 4.2	33.0 ± 3.8	36.4 ± 4.9	0.001
PA, mm	23.5 ± 2.8	23.0 ± 2.6	26.0 ± 3.0	<0.001
IVC, mm	15.5 ± 3.8	15.4 ± 3.7	16.0 ± 4.3	0.572
RVLS, %	23.5 ± 4.7	24.4 ± 4.4	18.5 ± 3.1	<0.001
RVFAC, %	45.8 ± 6.1	46.5 ± 5.7	41.6 ± 6.5	0.002
TAPSE, mm	22.9 ± 3.6	23.2 ± 3.5	21.0 ± 3.3	0.016
S′, cm/s	13.6 ± 2.4	13.7 ± 2.5	12.9 ± 1.9	0.223
Moderate to severe TR	8 (6.7)	7 (6.7)	1 (5.6)	0.839
PASP, mm Hg	31 (24–45)	28 (24–36)	48 (40–55)	0.042

Values are mean ± SD, n (%), or median (interquartile range). The p values comparing survivors and nonsurvivors are from chi-square test, Fisher exact test, or Mann-Whitney *U* test; p values <0.05 were considered to indicate statistical significance. RVLS values are absolute values.

Abbreviations as in Table 2.

lowest among patients with RVLS ≥25.5% ($p < 0.001$) (Central Illustration). When stratified by cutoff values, RVLS lower than 23% was associated with higher mortality ($p < 0.001$) (Central Illustration). It also clearly revealed that survival significantly declined with worsening TAPSE and RVFAC (Figures 4A and 4B).

A univariate Cox regression analysis showed that male sex (hazard ratio [HR]: 4.49; 95% confidence interval [CI]: 1.48 to 13.66; $p = 0.008$), ARDS (HR: 10.31; 95% CI: 2.98 to 35.63; $p < 0.001$), RVLS (HR: 1.45; 95% CI: 1.26 to 1.67; $p < 0.001$), RVFAC (HR: 0.88; 95% CI: 0.81 to 0.95; $p = 0.002$), and TAPSE (HR: 0.86; 95% CI: 0.76 to 0.97; $p = 0.018$) were associated with higher risk for mortality (Table 4). However, age, comorbidity, creatine kinase muscle-brain, hypersensitive troponin I, moderate to severe TR, angiotensin-converting enzyme inhibitor or angiotensin II receptor blocker therapy, S′, and LVEF were not predictive of mortality in univariate analysis. In multivariate Cox analysis models, ARDS continued to be of prognostic value. RVLS (HR: 1.33; 95% CI: 1.15 to 1.53; $p < 0.001$), RVFAC (HR: 0.90; 95% CI: 0.83 to 0.98; $p = 0.017$), and TAPSE (HR: 0.88; 95% CI: 0.78 to 0.99; $p = 0.044$) were independent predictors of higher mortality (Table 4). The model with RVLS (AIC = 129, C-index = 0.89) was the best in predicting mortality compared with those with RVFAC (AIC = 142, C-index = 0.84), TAPSE (AIC = 144, C-index = 0.83), and traditional risk factors (AIC = 146, C-index = 0.82).

REPRODUCIBILITY. The intraobserver and interobserver reproducibility of RVLS was excellent, as reflected by high ICC (intraobserver: 0.95; interobserver: 0.91). Bland-Altman analysis demonstrated good intraobserver and interobserver agreement, with small bias (intraobserver: −0.33; interobserver: 0.70) and narrow limits of agreement (intraobserver: −2.19 to 1.54; interobserver: −3.08 to 4.49).

DISCUSSION

To our knowledge, this is the first study to comprehensively evaluate the prognostic value of RV function using conventional echocardiography and 2D STE in patients with COVID-19. Patients with the greatest degree of RV strain impairment were more likely to have higher heart rates; more high-flow oxygen and invasive mechanical ventilation therapy; higher incidence of acute heart injury, ARDS, and deep vein thrombosis; and higher mortality. Compared with survivors, nonsurvivors had enlarged right heart chambers, diminished RV function, and elevated PASP. More important, RVLS was able to predict higher risk for mortality in patients with COVID-19, independently of and incrementally to other

FIGURE 2 Distribution of RVLS in Patients With COVID-19

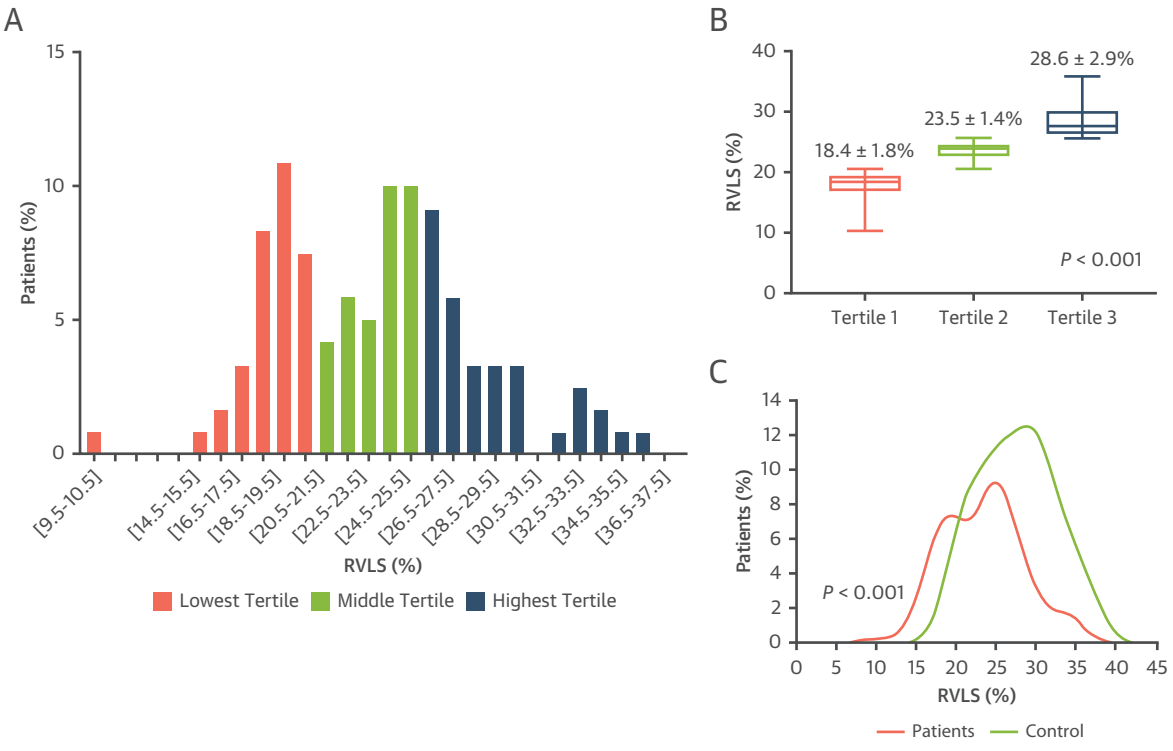

(A) Distribution of right ventricular longitudinal strain (RVLS) in patients with coronavirus disease-2019 (COVID-19) (**blue**, highest tertile; **green**, middle tertile; **red**, lowest tertile). **(B)** Tukey box-and-whisker plots of RVLS values in patients with COVID-19 according to the tertiles. **(C)** Distribution of RVLS in patients with COVID-19 **(red)** and healthy control subjects **(green)**. RVLS values are absolute values.

echocardiographic parameters. Therefore, a comprehensive assessment of RV function using 2D STE may be essential for risk stratification in patients with COVID-19.

PROGNOSIS OF RV FUNCTION IN COVID-19 PATIENTS. It is significant to recognize patients with COVID-19 at higher risk for poor outcomes who might benefit from vigilant monitoring. Several risk factors for poor prognosis have been identified in SARS-CoV-2 infection (16,17). The roles of the previously described prognostic markers, in particular ARDS and male sex, were confirmed in the present study. Furthermore, our study revealed important additional prognostic value of RV dysfunction. Most notably, the additional prognostic value of RVLS was substantial, independent of LV systolic functional index, which failed to predict mortality in patients with COVID-19. This is consistent with a previous study of LV performance in severe acute respiratory syndrome, showing that only subclinical LV diastolic impairment was observed in patients with severe acute respiratory syndrome (18). Nevertheless, the prognostic value of RV function was not yet explored in the study of severe acute respiratory syndrome.

RV dysfunction is related to significant morbidity and mortality in a variety of cardiovascular diseases (9,10,19,20). Indeed, in the present study, nonsurvivors displayed RV dilation and dysfunction. It has been reported that SARS-CoV-2 infection could cause both pulmonary and systemic inflammation, which may contribute to RV failure through RV overload and direct damage to cardiomyocytes (17,21). Similarly, in 42 patients with moderate to severe ARDS, Lazzeri et al. (22) demonstrated that troponin release can be related to RV dysfunction, thus emphasizing the clinical role of RV function (22). Moreover, although sharing considerable similarities, myocardial injury and cardiac insufficiency were more frequently reported in patients with COVID-19 than in those with severe acute respiratory syndrome (17,23). Therefore, assessment of RV function and recognition its prognostic significance is necessary in patients with COVID-19. RV

FIGURE 3 Receiver-Operating Characteristic Curves of RVLS, FAC, and TAPSE for Adverse Clinical Outcome

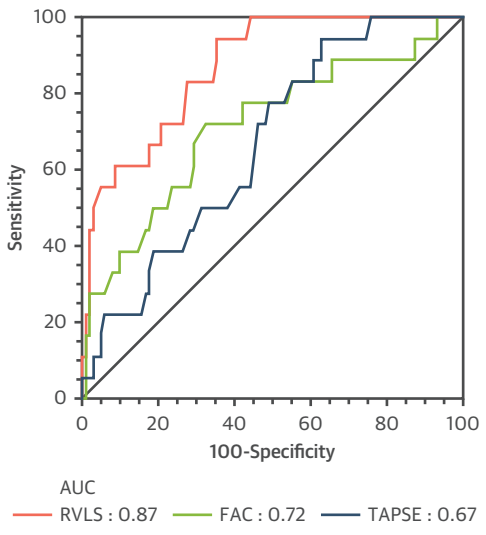

FAC = fractional area change; RVLS = right ventricular longitudinal strain; TAPSE = tricuspid annular plane systolic excursion.

dysfunction is not only a sign of increased pulmonary pressures but also directly contributes to cardiac insufficiency.

EVALUATION OF RV FUNCTION USING ECHOCARDIOGRAPHY. Although cardiac magnetic resonance remains the gold standard for quantifying RV function (24), in our study, the highly contagious nature of COVID-19 and patients' inability to hold their breath for a short time limited the application of cardiac magnetic resonance. Echocardiography is more widely used in daily practice. In clinical practice, it is routine to evaluate RV function using conventional echocardiographic parameters recommended by guidelines (14), which include TAPSE, RVFAC, and S′. However, each index has its own limitations. TAPSE and S′ represent only the longitudinal movement of the basal segment of the RV free wall and may fail to accurately reflect the entire RV performance. RVFAC is dependent on imaging plane, causing considerable interobserver and intraobserver variability in patients with suboptimal endocardial definition. In particular, the insufficient image quality in some patients with COVID-19 limits the accuracy of RVFAC measurement. Recently, 2D STE has been recommended as a superior method for assessment of RV performance, which has the advantage of being angle independent. Moreover, it can detect RV dysfunction more accurately and sensitively than TAPSE or RVFAC. Prior studies have revealed the prognostic utility of RVLS in various clinical settings (5,25,26).

Importantly, we demonstrated the superiority of RVLS over conventional RV functional parameters in identifying associations with outcomes. These findings were in keeping with the study of Carluccio et al. (5), which demonstrated that RVLS provided incremental prognostic information and enhanced risk stratification in patients with heart failure with preserved TAPSE. The superiority of RVLS may be related to several reasons. First, RVLS includes the whole RV free wall (basal, mid, and apical segments), contrary to TAPSE and S′, which assess only basal longitudinal

FIGURE 4 Kaplan-Meier Survival Curves Showing the Association of Higher Mortality and Right Ventricular Function

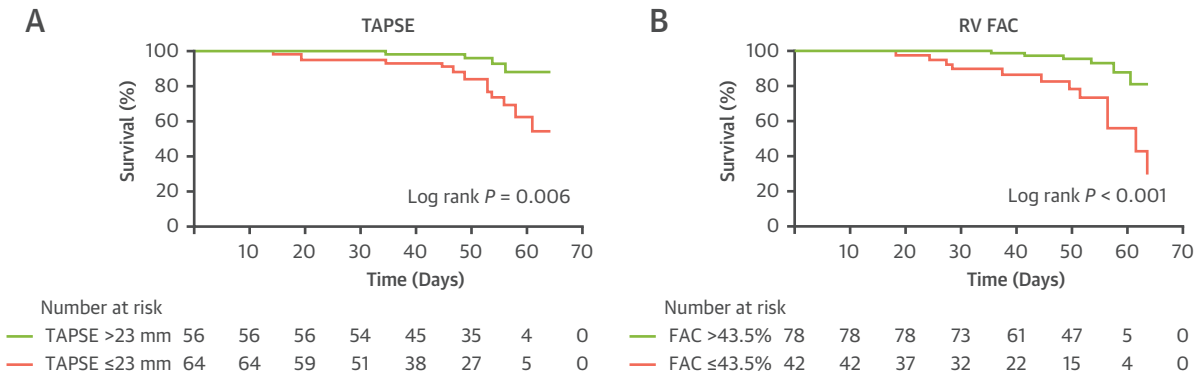

(A) Kaplan-Meier curve of survival in patients stratified by the cutoff value of tricuspid annular plane systolic excursion (TAPSE). **(B)** Kaplan-Meier curve of survival in patients stratified by the cutoff value of right ventricular fractional area change (FAC).

CENTRAL ILLUSTRATION **Association of Right Ventricular Longitudinal Strain and Mortality in Patients With COVID-19**

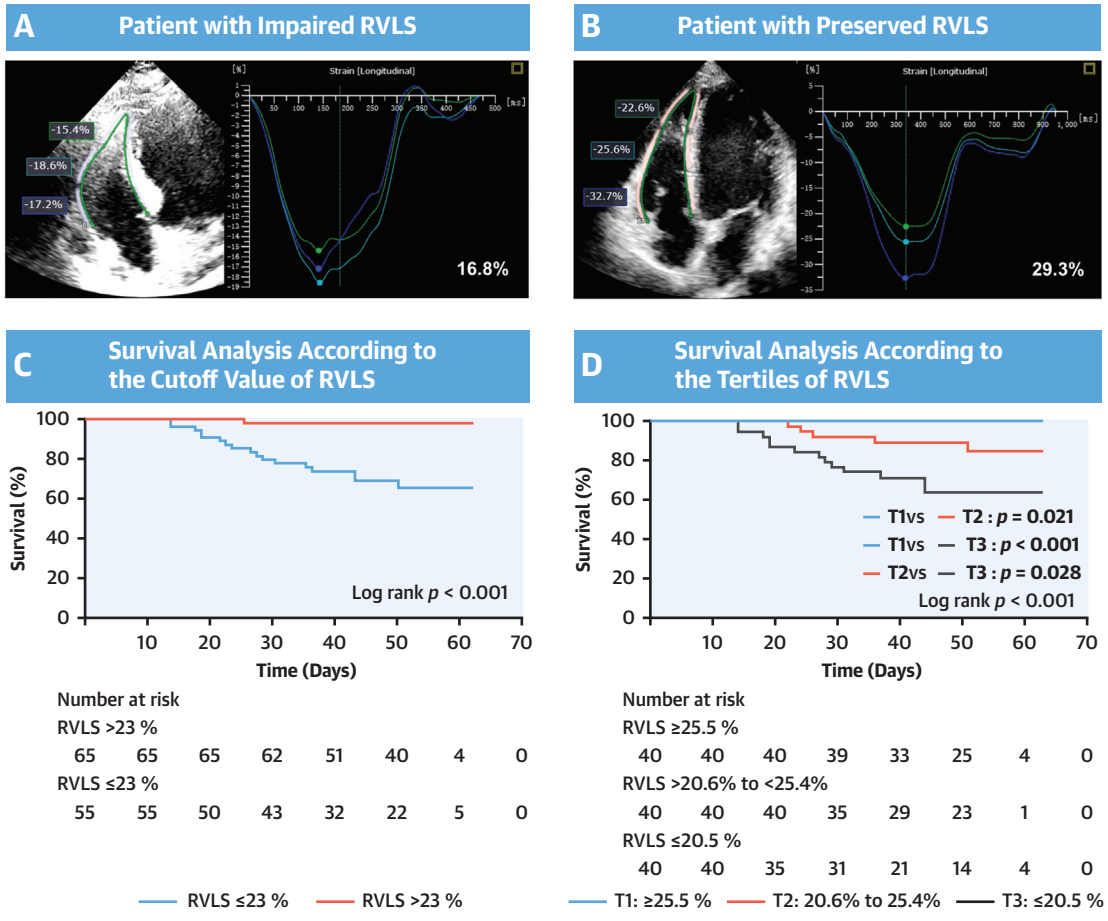

Li, Y. et al. J Am Coll Cardiol Img. 2020;13(11):2287-99.

In the **upper panel**, examples of strain plot of right ventricular longitudinal strain (RVLS) are shown: **(A)** a 42-year-old patient with impaired RVLS (16.8%), who died of coronavirus disease-2019 17 days after the echocardiographic examination; and **(B)** a 57-year-old patient with preserved RVLS (29.3%), who did not experience an event during 61 days of follow-up. In the **lower panel**, survival curves for all-cause mortality are shown **(C)** according to the cutoff value of RVLS (23%) and **(D)** according to tertiles of RVLS (≤20.5%, 20.6% to 25.4%, and ≥25.5%). RVLS values are absolute values.

motion. Furthermore, by tracking the myocardium throughout the cardiac cycle, RVLS can easily identify the maximal and minimal values of deformation, whereas RVFAC acquisition depends on end-diastole and end-systole frames. Finally, RVLS has been considered as a strong prognostic indicator for various cardiovascular diseases.

CLINICAL IMPLICATIONS. Our data demonstrated that RVLS was a powerful and independent predictor of higher mortality, providing additive predictive value over other echocardiographic parameters in patients with COVID-19. Accordingly, the present study revealed the important clinical implication of RVLS, as it can be easily obtained during bedside echocardiography. This suggests that evaluation of RV function using conventional echocardiographic measurements (i.e., RVFAC and TAPSE) should be complemented by longitudinal strain analysis to identify patients at higher risk for poor outcomes.

STUDY LIMITATIONS. Although our study was a cohort of homogenous and consecutive patients who were hospitalized with COVID-19, it was limited by being a single-center study with a relatively limited

TABLE 4 Predictors of Mortality In Patients With Covid-19 by Cox Proportional Hazard Model

	Univariate Cox Regression		Model 1 Gender + ARDS		Model 2 Gender + ARDS + TAPSE		Model 3 Gender + ARDS + RVFAC		Model 4 Gender + ARDS + RVLS	
	HR (95% CI)	p Value	HR (95% CI)	p Value	HR (95% CI)	p Value	HR (95% CI)	p Value	HR (95% CI)	p Value
Age	1.02 (0.99–1.06)	0.257								
Male	4.49 (1.48–13.66)	0.008	3.31 (1.08–10.13)	0.036		0.060	3.39 (1.10–10.41)	0.033		0.059
Hypertension	2.51 (0.97–6.47)	0.057								
Diabetes mellitus	0.41 (0.06–3.09)	0.387								
Coronary artery disease	2.93 (0.97–8.92)	0.058								
Malignancy	2.01 (0.46–8.76)	0.354								
ARDS	10.31 (2.98–35.63)	<0.001	8.65 (2.48–30.10)	0.001	6.78 (1.86–24.71)	0.004	6.63 (1.87–23.54)	0.003	4.47 (1.25–16.03)	0.021
CK-MB	1.02 (0.99–1.05)	0.208								
hs-TNI	0.99 (0.98–1.01)	0.580								
LVEF	1.07 (0.99–1.15)	0.115								
RVLS	1.45 (1.26–1.67)	<0.001							1.33 (1.15–1.53)	<0.001
RVFAC	0.88 (0.81–0.95)	0.002					0.90 (0.83–0.98)	0.017		
TAPSE	0.86 (0.76–0.97)	0.018			0.88 (0.78–0.99)	0.044				
S′	0.88 (0.72–1.08)	0.215								
Moderate to severe TR	1.03 (0.14–7.72)	0.979								
ACE inhibitor/ARB	0.80 (0.11–6.03)	0.831								
AIC	–	–	146		144		142		129	
C-index	–	–	0.82*		0.83		0.84*		0.89*	

*Values of $p < 0.05$ were considered to indicate statistical significance.

AIC = Akaike information criterion; CI = confidence interval; HR = hazard ratio; other abbreviations as in Figures 1 and 2.

sample size. Our hospital is among the hardest hit hospitals by the COVID-19 in Wuhan, thus the patients we included may not represent the populations in other areas. Moreover, we enrolled patients who were hospitalized with COVID-19, and asymptomatic patients who had not been admitted to the hospital were not included. Considering the wide clinical spectrum of SARS-CoV-2 infection, our findings may not be applicable to the entire COVID-19 population. Therefore, future multicenter studies with larger sample sizes are needed to determine the prognostic value of RVLS in patients with COVID-19. Additionally, we excluded 24 patients because of poor image quality precluding strain analysis, which limits the generalizability of our results. Also, our results pertain only to the software used in our study and may not apply to other software algorithms, because the 2D speckle-tracking echocardiographic parameters are hampered by the intervendor variability. We used RV free-wall longitudinal strain instead of global RV strain, because a simultaneous echocardiographic catheterization study demonstrated that free-wall longitudinal strain might better reflect RV function than global RV strain (27). Moreover, the relationship between LV and RV function could not be explored in the present study, as RV function could be affected by subclinical LV dysfunction. Furthermore, obese patients were uncommon in our study, as obesity is preliminarily considered as a high risk factor.

CONCLUSIONS

Our study demonstrates that RVLS is an independent determinant of outcomes in patients with COVID-19. Importantly, this index may have additional predictive value over other echocardiographic parameters. Therefore, evaluation of RV function should be implemented by investigation of RVLS for risk stratification in patients with COVID-19.

AUTHOR RELATIONSHIP WITH INDUSTRY

This work was supported by the National Natural Science Foundation of China (grants 81727805, 81922033, and 81401432). The authors have reported that they have no relationships relevant to the contents of this paper to disclose.

ADDRESS FOR CORRESPONDENCE: Dr. Li Zhang, Huazhong University of Science and Technology, 1277 Jiefang Avenue, Wuhan 430022, China. E-mail: zli429@hust.edu.cn. OR Dr. Mingxing Xie, 1277 Jiefang Avenue, Wuhan 430022, China. E-mail: xiemx@hust.edu.cn.

PERSPECTIVES

COMPETENCY IN PATIENT CARE AND PROCEDURAL SKILLS: RVLS is a powerful and independent predictor of higher mortality, providing additive predictive value over other echocardiographic parameters in patients with COVID-19. Our study demonstrated that comprehensive assessment of RV function by 2D STE may be essential for risk stratification in patients with COVID-19.

TRANSLATIONAL OUTLOOK: Future multicenter studies are needed to verify the value of 2D STE using different software for risk stratification of patients with COVID-19.

REFERENCES

1. Guo T, Fan Y, Chen M, et al. Cardiovascular implications of fatal outcomes of patients with coronavirus disease 2019 (COVID-19). JAMA Cardiol 2020;5:811–8.

2. Shi S, Qin M, Shen B, et al. Association of cardiac injury with mortality in hospitalized patients with COVID-19 in Wuhan, China. JAMA Cardiol. JAMA Cardiol 2020;5:802-10.

3. Huang C, Wang Y, Li X, et al. Clinical features of patients with 2019 novel coronavirus in Wuhan, China. Lancet 2020;395:497-506.

4. Yang X, Yu Y, Xu J, et al. Clinical course and outcomes of critically ill patients with SARSCoV-2 pneumonia in Wuhan, China: a single-centered, retrospective, observational study. Lancet. Respir Med 2020;8:475-81.

5. Carluccio E, Biagioli P, Alunni G, et al. Prognostic value of right ventricular dysfunction in heart failure with reduced ejection fraction: superiority of longitudinal strain over tricuspid annular plane systolic excursion. Circ Cardiovasc Imaging 2018;11:e006894.

6. Mor-Avi V, Lang RM, Badano LP, et al. Current and evolving echocardiographic techniques for the quantitative evaluation of cardiac mechanics: ASE/EAE consensus statement on methodology and indications endorsed by the Japanese Society of Echocardiography. Eur J Echocardiogr 2011;12:167-205.

7. Longobardo L, Suma V, Jain R, et al. Role of two-dimensional speckle-tracking echocardiography strain in the assessment of right ventricular systolic function and comparison with conventional parameters. J Am Soc Echocardiogr 2017;30:937-46.e6.

8. Li Y, Xie M, Wang X, et al. Impaired right and left ventricular function in asymptomatic children with repaired tetralogy of Fallot by two-dimensional speckle tracking echocardiography study. Echocardiography 2015;32:135-43.

9. Xie M, Li Y, Cheng TO, et al. The effect of right ventricular myocardial remodeling on ventricular function as assessed by two-dimensional speckle tracking echocardiography in patients with tetralogy of Fallot: a single center experience from China. Int J Cardiol 2015;178:300-7.

10. Park SJ, Park JH, Lee HS, et al. Impaired RV global longitudinal strain is associated with poor long-term clinical outcomes in patients with acute inferior STEMI. J Am Coll Cardiol Img 2015;8:161-9.

11. Motoki H, Borowski AG, Shrestha K, et al. Right ventricular global longitudinal strain provides prognostic value incremental to left ventricular ejection fraction in patients with heart failure. J Am Soc Echocardiogr 2014;27:726-32.

12. World Health Organization. Clinical management of severe acute respiratory infection when COVID-19 is suspected. Available at: https://www.who.int/publications-detail/clinical-management-of-severe-acute-respiratory-infection-when-novel-coronavirus-(ncov)-infection-is-suspected. Accessed January 28, 2020.

13. World Medical Association. World Medical Association Declaration of Helsinki: ethical principles for medical research involving human subjects. JAMA 2013;310:2191–4.

14. Rudski LG, Lai WW, Afilalo J, et al. Guidelines for the echocardiographic assessment of the right heart in adults: a report from the American Society of Echocardiography endorsed by the European Association of Echocardiography and the Canadian Society of Echocardiography. J Am Soc Echocardiogr 2010;23:685–713.

15. Lang RM, Badano LP, Mor-Avi V, et al. Recommendations for cardiac chamber quantification by echocardiography in adults: an update from the American Society of Echocardiography and the European Association of Cardiovascular Imaging. J Am Soc Echocardiogr 2015;28:1-39.e14.

16. Chen N, Zhou M, Dong X, et al. Epidemiological and clinical characteristics of 99 cases of 2019 novel coronavirus pneumonia in Wuhan, China: a descriptive study. Lancet 2020;395:507–13.

17. Chen T, Wu D, Chen HL, et al. Clinical characteristics of 113 deceased patients with coronavirus disease 2019: retrospective study. BMJ 2020;368:m1295.

18. Li SS, Cheng CW, Fu CL, et al. Left ventricular performance in patients with severe acute respiratory syndrome: a 30-day echocardiographic follow-up study. Circulation 2003;108:1798–803.

19. Alashi A, Mentias A, Abdallah A, et al. Incremental prognostic utility of left ventricular global longitudinal strain in asymptomatic patients with significant chronic aortic regurgitation and preserved left ventricular ejection fraction. J Am Coll Cardiol Img 2017;11:673–82.

20. Houard L, Benaets MB, de Meester de Ravenstein C, et al. Additional prognostic value of 2D right ventricular speckle-tracking strain for prediction of survival in heart failure and reduced ejection fraction: a comparative study with cardiac magnetic resonance. J Am Coll Cardiol Img 2019;12:2373–85.

21. Li B, Yang J, Zhao F, et al. Prevalence and impact of cardiovascular metabolic diseases on COVID-19 in China. Clin Res Cardiol 2020;109:531–8.

22. Lazzeri C, Bonizzoli M, Cozzolino M, et al. Serial measurements of troponin and echocardiography in patients with moderate-to-severe acute respiratory distress syndrome. J Crit Care 2016;33:132–6.

23. Liu CL, Lu YT, Peng MJ, et al. Clinical and laboratory features of severe acute respiratory syndrome vis-a-vis onset of fever. Chest 2004;126:509–17.

24. D'Ascenzi F, Anselmi F, Piu P, et al. Cardiac magnetic resonance normal reference values of biventricular size and function in male athlete's heart. J Am Coll Cardiol Img 2019;12:1755–65.

25. Mast TP, Taha K, Cramer MJ, et al. The prognostic value of right ventricular deformation imaging in early arrhythmogenic right ventricular cardiomyopathy. J Am Coll Cardiol Img 2019;12:446–55.

26. Medvedofsky D, Koifman E, Jarrett H, et al. Association of right ventricular longitudinal strain with mortality in patients undergoing transcatheter aortic valve replacement. J Am Soc Echocardiogr 2020;33:452–60.

27. Cameli M, Bernazzali S, Lisi M, et al. Right ventricular longitudinal strain and right ventricular stroke work index in patients with severe heart failure: left ventricular assist device suitability for transplant candidates. Transplant Proc 2012;44.2013–5.

KEY WORDS COVID-19, right ventricular function, SARS-CoV-2, speckle tracking echocardiography, strain